Kinetic Modeling of Xylose Oligomer Degradation during Pretreatment in Dilute Acid or in Water

ARTICLE *in* INDUSTRIAL & ENGINEERING CHEMISTRY RESEARCH · FEBRUARY 2014

Impact Factor: 2.59 · DOI: 10.1021/ie403722d

I&EC research
Industrial & Engineering Chemistry Research

Article

pubs.acs.org/IECR

Kinetic Modeling of Xylose Oligomer Degradation during Pretreatment in Dilute Acid or in Water

Ching-Shuan Lau,[†] Greg J. Thoma,[‡] Edgar C. Clausen,[‡] and Danielle J. Carrier*[,†]

[†]Department of Biological and Agricultural Engineering, University of Arkansas, 203 Engineering Hall, Fayetteville, Arkansas 72701, United States

[‡]Ralph E. Martin Department of Chemical Engineering, University of Arkansas, 3202 Bell Engineering Center, Fayetteville, Arkansas 72701, United States

ABSTRACT: Hemicellulose in lignocellulosic biomass can be depolymerized into fermentable sugars using dilute acid pretreatment. However, this pretreatment results in the production of degradation compounds that inhibit subsequent hydrolysis and fermentations steps. Understanding the effect of pretreatment processing parameters on hemicellulose depolymerization could possibly result in minimization of degradation compounds. We report on depolymerization studies of in-house-purified birchwood xylan oligomers, namely, xylobiose, xylotriose, and xylotetraose, and on commercially available xylose, furfural, and formic acid. On the basis of the current study, the optimum hydrolysis conditions were at temperatures between 120 and 130 °C and acid concentrations between 0.6 and 1.0 v/v%, where carbohydrate monomers were maximized, and degradation products were minimized. These results indicate that it is possible to improve hemicellulose-to-xylose conversion efficiency while minimizing degradation product generation, reducing detoxification requirements.

INTRODUCTION

The carbohydrate components of cellulosic feedstock, cellulose and hemicellulose, need to be deconstructed into their monomeric sugars in order to be used for biofuels or manufacture of other biobased products. To release sugars from the tightly interlinked plant cell wall structure, pretreatment and enzymatic hydrolysis—bioprocessing operations are required. The resulting sugar stream is then fermented with different microorganisms, depending on the targeted product. There are a number of available pretreatment technologies, such as, but not limited to, ammonia fiber explosion, ionic liquids, hot water hydrolysis, or dilute acid. Despite its many drawbacks, dilute acid pretreatments are most likely to be adopted at the deployment stage because of their low cost and ease of use.[1] Dilute acid pretreatments are effective in releasing hemicellulose from the cell wall and, thus, have been used as pretreatment for a variety of feedstocks, ranging from hardwoods to grasses and agricultural residues.[2]

In addition to producing monomeric sugars, dilute acid pretreatments are unfortunately conducive to the generation of byproducts, which pose problems for downstream enzymatic hydrolysis and fermentation.[3] Specifically, during dilute acid hydrolysis, hemicellulose depolymerizes into xylose oligomers of different degree of polymerization (DP), before forming xylose monomers.[2,4−6] In the presence of acid, xylose monomers degrade further into furfural and formic acid,[7] both of which are inhibitory to enzymatic hydrolysis[8,9] and to yeast during the downstream sugar-to-ethanol fermentation process.[10] Furthermore, insufficient hydrolysis of hemicellulose results in a high concentration of xylose oligomers, which inhibit the enzymatic hydrolysis of cellulose and xylan.[4,11] Moreover, byproducts formed by the degradation of xylose are not stable. As an example, furfural can further degrade into formic acid[12] and humin.[13,14] Formic acid can also form furfural via autocatalytic mechanisms[14,15] and decompose into carbon dioxide, carbon monoxide, hydrogen, and water.[16,17] To produce a high-quality sugar stream, the effect of dilute acid pretreatment processing parameters on byproduct formation must be understood such that effective trade-offs can be established between sugar maximization and inhibitory product minimization.

In a pioneering study, Kamiyama and Sakai[18] described the depolymerization of soluble oligomers to degradation products. In a further study, Kumar and Wyman[6] hydrolyzed xylose oligomer reference standards at 160 °C and at five different pH conditions, from which they developed a depolymerization model. The depolymerization model in both studies lumped together all degradation productions and calculated the degradation as a lost compound. In another approach adopted by Morinelly et al.,[19] aspen, balsam, and switchgrass hemicellulose were depolymerized in 0.25−0.75 wt % sulfuric acid. The reactions were assumed to follow first-order kinetics, but the resulting fit between the developed model and experimental data was not optimal, possibly due to the use of a very complex experimental hydrolyzate, containing a plethora of hydrolyzed compounds.[19] Kim et al.[20] studied the depolymerization of hardwood-derived oligomers under different acid regimes to degradation products, using a first-order kinetic reaction model. To simplify their model, Kim et al.[20] lumped oligomers together but accounted for individual degradation products. To produce a high-quality fermentable sugar stream from cellulosic biomass, it is imperative that hemicellulose depolymerization is understood and modeled, meaning that both oligomer

Received: November 3, 2013
Revised: January 14, 2014
Accepted: January 16, 2014

   dx.doi.org/10.1021/ie403722d | *Ind. Eng. Chem. Res.* XXXX, XXX, XXX−XXX

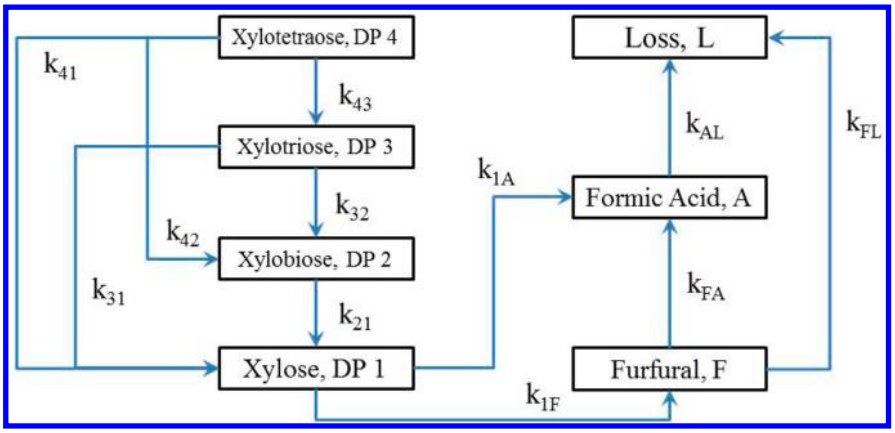

Figure 1. The degradation model of xylose oligomers. k_1, k_2, k_3, k_4, k_F, and k_A are the overall degradation rate constants for DP 1, DP 2, DP 3, DP 4, furfural, and formic acid, respectively, in min^{-1}, and k_{41}, k_{42}, k_{31}, k_{21}, k_{1F}, k_{1A}, and k_{FA} are the formation rate constants of DP 1 from DP 4, DP 2 from DP 4, DP 1 from DP 3, DP 1 from DP 2, furfural from DP 1, formic acid from DP 1, and formic acid from furfural, respectively, in min^{-1}. The rate constants k_{FL} and k_{AL} are the decomposition rate of furfural and formic acid, respectively. The term loss represents products from formic acid and furfural degradation, such as carbon dioxide, carbon monoxide, hydrogen, water, and humin, all of which were not measured in this experiment.

depolymerization and byproduct formation are described. Moreover, the effect of classical processing parameters, time, pH, and temperature, on hemicellulose depolymerization must be appreciated such that useable sugar streams, with minimal byproduct concentrations, are generated. No existing kinetic study accounts simultaneously for individual oligomers, monomer, and byproducts during depolymerization.

Xylose oligomers, which are abundant from biomass sources, are important intermediates during hemicellulose depolymerization. Current and proposed methods for purification of xylose oligomers include hot water extraction, membrane filtration, and purification using centrifugal partition chromatography (CPC). In a previous paper, we reported on the purification and production of authentic xylose oligomers.[21] Experiments were conducted with these in-house-produced oligomers to describe their depolymerization, using a range of pretreatment conditions. The authors recognize that the range of conditions in the current study do not represent realistic processing conditions but are important to describe the rate of formation for monomeric sugars and ensuing byproducts. Having determined the effect of temperature and acid concentration on these rates, ideal hydrolysis conditions for xylose accumulation can be suggested.

In this study, the formation and degradation of xylose oligomers were monitored and their depolymerization processes were represented by first-order kinetics. Arrhenius relations were also formulated. The developed model was useful in determining the effect of temperature and pH on the overall yield of xylose monomer and ensuing degradation products, establishing ranges in which processing parameter trade-offs could occur.

MATERIALS AND METHODS

Materials. Birchwood xylan, xylose (DP 1), and furfural were acquired from Sigma-Aldrich (St. Louis, MO). Xylobiose (DP 2), xylotriose (DP 3), xylotetraose (DP 4), xylopentaose (DP 5), and xylohexaose (DP 6) reference compounds were purchased from Megazyme (Wicklow, Ireland). HPLC grade methanol and sulfuric acid were procured from EMD Chemicals (Gibbstown, NJ). Butanol, calcium carbonate, and formic acid were obtained from Avantor Performance Materials, Inc. (Center Valley, PA), Fisher Scientific (Fair Lawn, NJ), and EM Science (Gibbstown, NJ), respectively. Water was purified with a Direct-Q system (Millipore, Billerica, MA).

Purification of Xylose Oligomers. The purification of xylose oligomers was conducted using the solvent system of butanol:methanol:water in 5:1:4 volumetric ratio developed by Lau et al.[21] The CPC separation was performed using a CherryOne DS bench scale counter current chromatography (CCC) control system from Cherry Instruments (Chicago, IL), which utilized a CPC rotor from Armen Instruments (Saint-Avé, France). Detection was achieved using an ELSD (SofTA Corporation, Westminster, CO) setup with 50 psig air pressure of ultrapure nitrogen, a 25 °C spray chamber temperature, and a 55 °C drift tube temperature. The 250-mL rotor was first filled with lower phase, mainly water with methanol, at 10 mL/min with the rotor spinning at 500 rpm. Once the rotor was completely filled with the stationary phase, which took approximately 30 min, the CPC rotor speed was increased to 2300 rpm. At that point, the upper phase, mainly butanol with some methanol, was introduced into the CPC rotor at a flow rate of 8 mL/min. The mobile phase volume was determined once the upper phase exited the CPC rotor. A 30 mL xylan hydrolysate was injected into the 30 mL sample loop, which was then introduced into the CPC rotor, and this was selected as the beginning of the CPC fractionation experiment. The flow rate was set at 8 mL/min. Fractions were collected 75 min after the sample injection using a Foxy R1 fraction collector (Teledyne Isco, Lincoln, NE). The sample collection lasted for 125 min, with each fraction being collected over 1 min. At 165 min after the sample injection, the phases were reversed to begin the extrusion process. From the 200 min CPC run, the mobile and stationary phases were 132 and 118 mL, respectively, with the operating pressure at approximately 650 psig.

Hot Water and Acid Hydrolysis of Xylose Oligomers. The experiments were performed in thick-walled (interior diameter 14.22 mm, wall thickness 5.59 mm, and length 100 mm) stainless-steel reactors; the total chamber volume was 16 mL, to which 5 mL of CPC purified oligomers were added. The hydrolysis time began 75 s after the reactors were submerged in an industrial fluidized sand bath (Techne Ltd, Burlington, NJ). The 75 s delay time was determined as the time required for water to boil in the reactor tube, as measured with a

dx.doi.org/10.1021/ie403722d | Ind. Eng. Chem. Res. XXXX, XXX, XXX−XXX

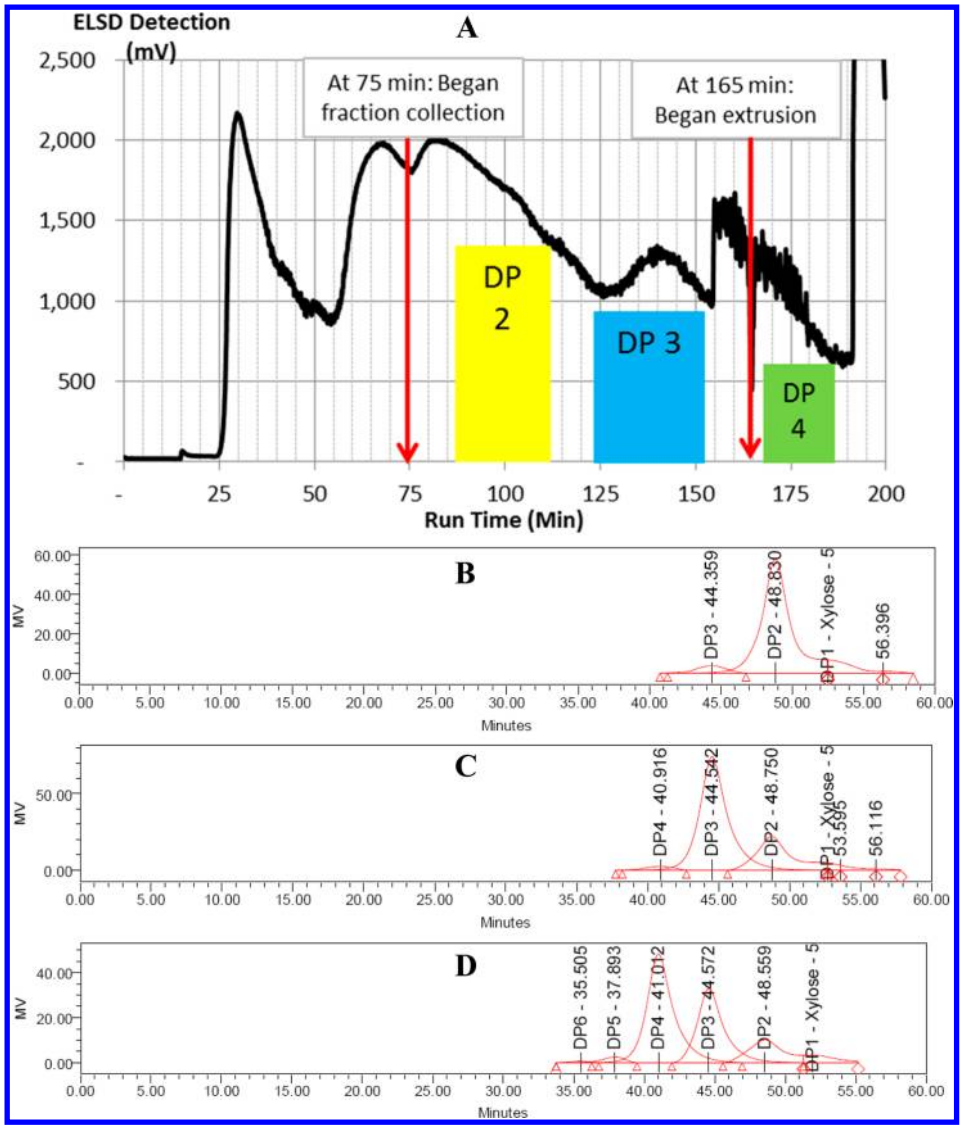

Figure 2. (A) Centrifugal partition chromatography chromatogram for hydrolyzed birchwood xylan. The CPC-fractionated xylose oligomers were detected by HPLC, as shown in (B) xylobiose (DP 2)-rich fraction, (C) xylotriose (DP 3)-rich fraction, and (D) xylotetraose (DP 4)-rich fraction.

thermometer. The sand bath was preheated to reach the desired experimental temperature. Experiments for formic acid, furfural, DP 1, and DP 2 were conducted at temperatures of 120, 160, and 200 °C and at sulfuric acid concentrations of 0 v/v% (pH 7.00), 0.1 v/v% (pH 1.43), and 1 v/v% (pH 0.43). Experiments for DP 3 were conducted at 160 °C with water and 0.1 and 1 v/v% sulfuric acid and at 200 °C in water and in 0.1 v/v% sulfuric acid. Experiments for DP 4 were conducted at 160 °C with water and 1 and 0.1 v/v% sulfuric acid and water at 200 °C. Each reactor was submerged into the sand bath for a set time and quenched by running tap water for 1 min to stop the reaction and to reduce the pressure. Each experimental condition was performed in duplicate. Once cooled, the reactors were opened, and the hydrolysate was transferred to glass tubes, neutralized with calcium carbonate, filtered through a 0.2-μm nylon syringe filter (National Scientific, Rockwood, TN), and analyzed for carbohydrates, formic acid, and furfural by HPLC as described by Djioleu et al.[22] and for oligomers as in Martin et al.[23] DP 2, DP 3, DP 4, DP 5, and DP 6 were used as retention time standards and constructing calibration curves.

Reaction Model. The xylose oligomers depolymerization model used in this study is presented in Figure 1. The constants k_1, k_2, k_3, k_4, k_F, k_A are the overall degradation rates of DP 1, DP 2, DP 3, DP 4, furfural, and formic acid, respectively, in min^{-1}. The constants k_{41}, k_{42}, k_{43}, k_{31}, k_{32}, k_{21}, k_{1F}, k_{1A}, and k_{FA} are the constants for the formation of DP 1 from DP 4, DP 2 from DP 4, DP 3 from DP 4, DP 1 from DP 3, DP 2 from DP 3, DP 1 from DP 2, furfural from DP 1, formic acid from DP 1, and formic acid from furfural, respectively, in min^{-1}. Lastly, k_{FL} and k_{AL} are the constants that represent the decomposition of furfural and formic acid to loss, respectively. According to the first-order kinetics, the reaction rate is

$$d[X]/dt = -k[X] \quad (1)$$

where [X] is the concentration of compound X in mmol/L, t is the hydrolysis time in min, and k is the rate of compound degradation in min^{-1}. Therefore, $d[X]/dt$ is the rate of change for compound X with respect to time. The assumptions made to develop the model were the following: (1) all degradation reactions followed first-order kinetics; (2) the reactions were irreversible, given the low concentration of compound; and (3)

dx.doi.org/10.1021/ie403722d | Ind. Eng. Chem. Res. XXXX, XXX, XXX−XXX

furfural was formed from DP 1, and the xylose oligomers, DP 2, DP 3, and DP 4, had to depolymerize to DP 1 before degrading into furfural. Combining eq 1 with the reactions presented in Figure 1, the mass balances for DP 1, DP 2, DP 3, DP 4, furfural, and formic acid are

$$d[X_1]/dt = -k_1[X_1] + k_{41}[X_4] + k_{31}[X_3] + 2k_{21}[X_2] \quad (2)$$

$$d[X_2]/dt = -k_2[X_2] + 2k_{42}[X_4] + k_{32}[X_3] \quad (3)$$

$$d[X_3]/dt = -k_3[X_3] + k_{43}[X_4] \quad (4)$$

$$d[X_4]/dt = -k_4[X_4] \quad (5)$$

$$d[X_F]/dt = -k_F[X_F] + k_{1F}[X_1] \quad (6)$$

$$d[X_A]/dt = -k_A[X_A] + k_{1A}[X_1] + k_{FA}[X_F] \quad (7)$$

where $[X_1]$, $[X_2]$, $[X_3]$, $[X_4]$, $[X_F]$, $[X_A]$ are the concentrations of DP 1, DP 2, DP 3, DP 4, furfural, and formic acid, respectively, in mmol/L.

The relationship between the overall degradation and the formation rates of individual compounds is summarized as follows:

$$k_1 = k_{1F} + k_{1A} \quad (8)$$

$$k_2 = k_{21} \quad (9)$$

$$k_3 = k_{31} = k_{32} \quad (10)$$

$$k_4 = k_{41}\ (=k_{43}) + k_{42} \quad (11)$$

$$k_F = k_{FA} + k_{FL} \quad (12)$$

$$k_A = k_{AL} \quad (13)$$

The expression of individual compound concentrations $[X_1]$, $[X_2]$, $[X_3]$, $[X_4]$, $[X_F]$, and $[X_A]$ with respect to time was performed using normal integrations, with the estimated values at nine hydrolysis conditions for DP 2, DP 1, furfural, and formic acid; five hydrolysis conditions for DP 3; and four hydrolysis conditions for DP 4. The calculated degradation or formation constants were used to compute the Arrhenius constants, as described by Kim et al.[20] and Saeman:[24]

$$k = k_0[H^+]^m \exp(-E/RT) \quad (14)$$

where k, k_0, $[H^+]$, m, E, R, and T are the first-order rate constant in min^{-1}, pre-exponential rate constant in min^{-1}, hydrogen ion concentration in mol/L, unitless acid concentration exponent, activation energy in kJ/mol, gas constant in kJ/mol/K, and the hydrolysis temperature in K, respectively.

Data Analysis. The overall degradation rate constants k_1, k_2, k_3, k_4, k_F, and k_A and the individual formation rate constants for k_{41}, k_{42}, k_{43}, k_{31}, k_{32}, k_{21}, k_{1F}, k_{1A}, and k_{FA} for each compound, as well as the estimation of Arrhenius constants, k_0, m, and E, were estimated by minimizing the differences between experimental and predicted data using the Excel Solver Routine.

Data Fitting. The experimental data were fitted to the reaction model described by eqs 2−13 by the sum of the squares method, as described by eq 15. Using this method, all data were given equal consideration, preventing bias. The calculated S value in eq 15 was maximized to obtain the optimum values for the individual degradation rates described by eqs 2−13.

R^2 method:

$$S = \sum\{1 - [(\text{predicted data} - \text{experimental data})^2 / (\text{experimental data} - \text{average of experimental data})^2]\} \quad (15)$$

RESULTS AND DISCUSSION

Hydrolysis of Xylose Oligomers, Monomer, and Byproducts. The evaporative light scattering detector (ELSD) chromatogram of the CPC fractionation xylose oligomers in butanol:methanol:water at a 5:1:4 volumetric ratio is presented in Figure 2. Xylose oligomers, namely, DP 2, DP 3, and DP 4, were produced at purity levels of 91, 71, and 49%, respectively. The purity of the CPC-purified oligomers was determined on the basis of the peak area of the targeted oligomer divided by the total peak area of DP 1 to DP 12, as determined by the HPLC analysis. The presence of these contaminants was accounted for in the developed kinetic model by setting the initial concentration of the contaminants to nonzero values and thus did not affect the model's utility in determining kinetic parameters through least-squares optimization.

Preliminary experiments showed that initial reactor loadings at concentrations between 6.7 and 33.3 mmol/L (1−5 g/L) yielded first-order reaction degradation rates (Figure 3).

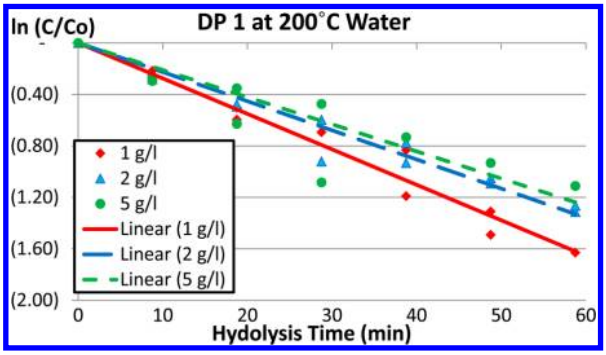

Figure 3. Degradation profile of DP 1 at 1, 2, and 5 g/L (6.7, 13.3, and 33.3 mmol/L) initial concentration in 200 °C water.

Moreover, the degradation rate constant of DP 1 was determined to be independent of initial DP 1 concentrations, as determined from the F-test analysis, confirming that the reaction was first-order.

The depolymerization of DP 4 is presented in Figure 4. For the 200 °C water (0 v/v% acid) hydrolysis condition, less than 15% of initial DP 4 remained after 40 min of hydrolysis. Among the four tested hydrolysis conditions, 160 °C water resulted in 13% of DP 4 remaining after 40 min. In comparison, in the most severe hydrolysis condition, 1 v/v% acid at 160 °C, all DP 4 was fully depolymerized within 5 min into a mixture of DP 3, DP 2, DP 1, furfural, and formic acid. Because of the rapid depolymerization rate, the highest observed concentrations of furfural were obtained with 1 v/v% sulfuric acid at 160 °C. Conversely, during slower depolymerization, such as with 160 °C water, 0.1 v/v% sulfuric acid at 160 °C, and 200 °C water, most of the initial DP 4 remained as xylose oligomers, namely, DP 2, DP 3, and DP 4. Specifically, 40, 51, and 31% of xylose oligomers remained in xylose equivalent moles, in water at 160 °C after 40 min, 0.1 v/v% sulfuric acid at 160 °C after 30 min, and water at 200 °C after 5 min, respectively.

dx.doi.org/10.1021/ie403722d | Ind. Eng. Chem. Res. XXXX, XXX, XXX−XXX

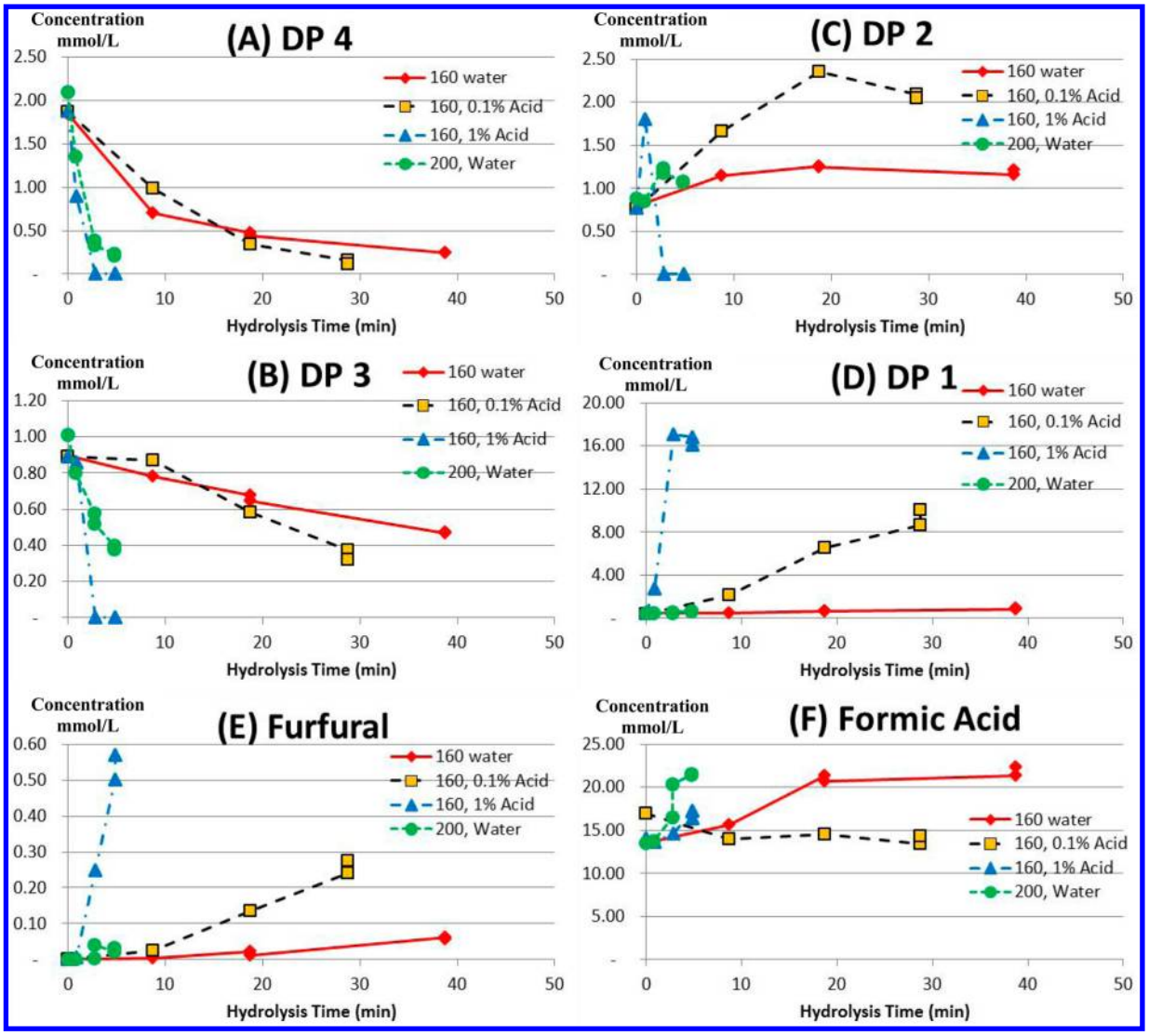

Figure 4. Hydrolysis of DP 4. The experimental data showing the molar concentration of (A) DP 4, (B) DP 3, (C) DP 2, (D) DP 1, (E) furfural, and (F) formic acid as a function of hydrolysis time during the hydrolysis of DP 4 in 160 °C water, 160 °C 0.1 v/v% sulfuric acid, 160 °C 1 v/v% sulfuric acid, and 200 °C water.

In a similar fashion, the study of the thermal degradation of DP 3 was conducted in 1, 0.1, and 0 v/v% acid at 160 °C and in 0.1 and 0 v/v% acid at 200 °C. Among the five hydrolysis conditions, 1 v/v% sulfuric acid at 160 °C and 0.1 v/v% sulfuric acid at 200 °C resulted in a complete depolymerization of DP 3 within 5 min of the hydrolysis, mainly into DP 1 and furfural. On the other hand, during the least severe hydrolysis condition, the hydrolysis with water at 160 °C, 34% of DP 3 remained after 40 min of hydrolysis. Interestingly, with 1 v/v% sulfuric acid at 160 °C, the degradation of formic acid was as fast as its accumulation; the concentration of formic acid remained below 2 mmol/L throughout the hydrolysis process.

The hydrolysis of DP 2 was conducted in nine different hydrolysis conditions: 1, 0.1, and 0 v/v% acid at 120 °C; 1, 0.1, and 0 v/v% acid at 160 °C; and 1, 0.1, and 0 v/v% acid at 200 °C. As expected, during the less severe hydrolysis conditions, 120 °C water and 0.1 v/v% sulfuric acid, as well as 160 °C water and 0.1 v/v% sulfuric acid, the concentrations of DP 2 remaining after 60 min of hydrolysis were 92%, 64%, 27%, and 1%, respectively. During hydrolysis at 120 °C 1 v/v% sulfuric acid, at 160 °C 1 v/v% sulfuric acid, and at 200 °C water 0.1 and 1 v/v% sulfuric acid, complete depolymerization of DP 2 was noted within 20 min. Although a high concentration of DP 1 at 12 mmol/L was initially observed during hydrolysis at 160 °C 1 v/v% sulfuric acid and at 200 °C 0.1 and 1 v/v% sulfuric acid, DP 1 was degraded within 20 min into furfural concentrations of 4.1, 3.5, and 4.9 mmol/L, respectively. Although DP 2 samples contained 9 mmol/L of formic acid at the onset of the experiments, hydrolysis conditions at 160 °C 1 v/v% sulfuric acid and at 200 °C 0.1 and 1 v/v% sulfuric resulted in almost no change in formic acid concentrations, where formic acid concentrations remained at 9 mmol/L. Less severe hydrolysis conditions in 200 °C water yielded 14 mmol/L, the highest detected concentration of formic acid.

Similar to DP 2, DP 1 also underwent dehydration at nine hydrolysis conditions, as shown in Figure 5. After 60 min of hydrolysis, all three experiments conducted at 120 °C resulted in a high survival rate of DP 1, as shown by 89%, 93%, and 93% of DP 1 remaining in 120 °C water, 0.1 v/v% sulfuric acid at 120 °C, and 1 v/v% sulfuric acid at 120 °C, respectively. In 200 °C or in 1 v/v% sulfuric acid at 160 °C, no more than 79% of DP 1 remained at the end of the reaction. On the other hand,

dx.doi.org/10.1021/ie403722d | Ind. Eng. Chem. Res. XXXX, XXX, XXX−XXX

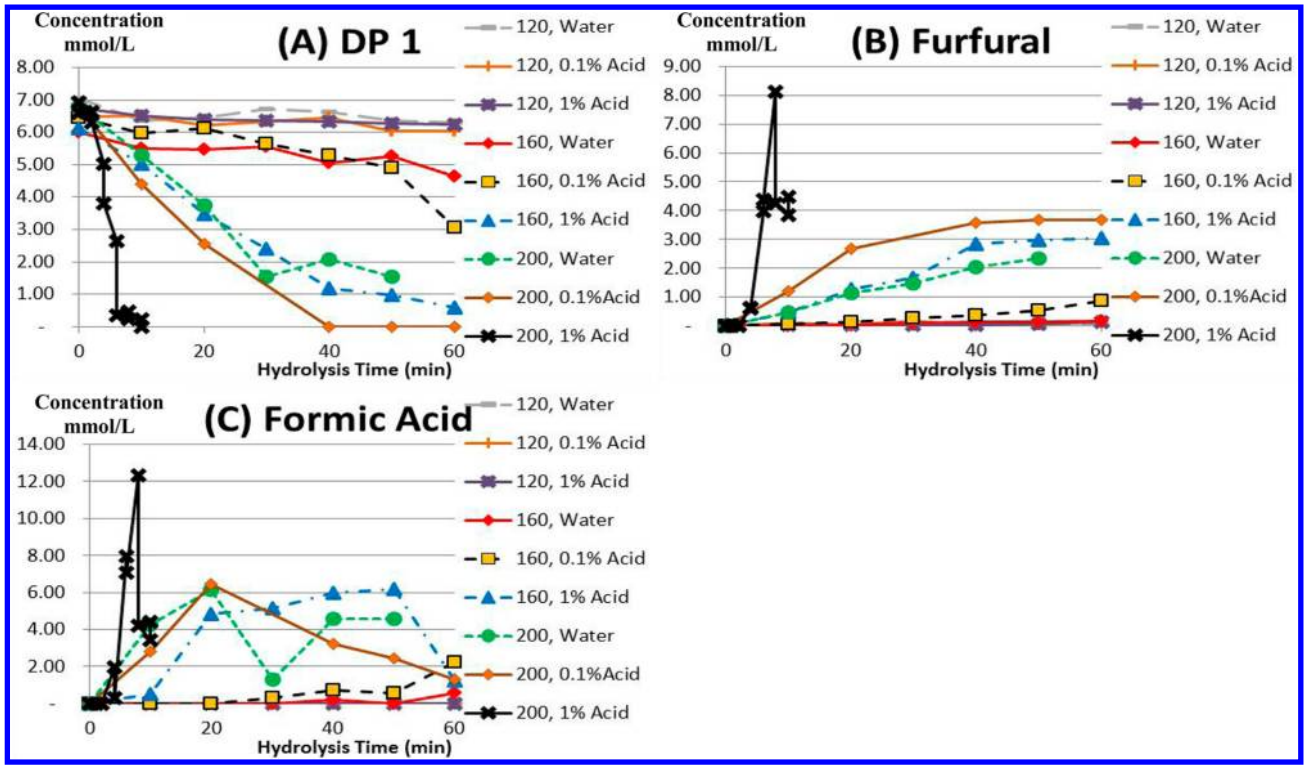

Figure 5. Hydrolysis of DP 1. The experimental data showing the molar concentration of (A) DP 1 (xylose), (B) furfural, and (C) formic acid as a function of hydrolysis time during the hydrolysis of DP 1 in 120 °C water, 120 °C 0.1 v/v% sulfuric acid, 120 °C 1 v/v% sulfuric acid, 160 °C water, 160 °C 0.1 v/v% sulfuric acid, 160 °C 1 v/v% sulfuric acid, 200 °C water, 200 °C 0.1 v/v% sulfuric acid, and 200 °C of 1 v/v% sulfuric acid.

Table 1. Summary of the Degradation Rate Constants Obtained in This Study[a]

	120 °C			160 °C			200 °C		
	water	0.1% acid	1% acid	water	0.1% acid	1% acid	water	0.1% acid	1% acid
k_1	0.0044	0.0013	0.0019	0.0054	0.0057	0.0363	0.2396	0.0343	0.3055
k_2	0.0003	0.0038	0.2513	0.0030	0.0439	1.0152	0.0414	0.2431	2.2762
k_3				0.0103	0.1048	1.9862	0.0681	0.4787	
k_4				0.0032	0.1049	3.8453	0.0161		
k_F	0.0014	0.0015	0.0026	0.0027	0.0014	0.0040	0.0044	0.0079	0.0154
k_A	0.0013	0.0015	0.0012	0.0004	0.0013	0.0008	0.0020	0.0020	0.0021
k_{41} (=k_{43})				0.0001	0.0699	3.8453	0.0026		
k_{42}				0.0031	0.0350	0.0000	0.0136		
k_{31} (=k_{32})				0.0103	0.1048	1.9862	0.0681	0.4787	
k_{21}	0.0003	0.0038	0.2513	0.0030	0.0439	1.0152	0.0414	0.2431	2.2762
k_{1F}	0.0001	0.0001	0.0005	0.0014	0.0020	0.0128	0.0112	0.0234	0.1428
k_{1A}	0.0043	0.0012	0.0014	0.0040	0.0037	0.0235	0.2284	0.0109	0.1627
k_{FA}	0.0014	0.0003	0.0025	0.0027	0.0014	0.0040	0.0038	0.0079	0.0154
k_{FL}	0.0000	0.0012	0.0000	0.0000	0.0000	0.0000	0.0005	0.0000	0.0000
k_{AL}	0.0013	0.0015	0.0012	0.0004	0.0013	0.0008	0.0020	0.0020	0.0021

[a]The constants k_1, k_2, k_3, k_4, k_F, and k_A are the overall degradation rates of DP 1, DP 2, DP 3, DP 4, furfural, and formic acid, respectively, in min^{-1}. The constants k_{41}, k_{42}, k_{43}, k_{31}, k_{32}, k_{21}, k_{1F}, k_{1A}, and k_{FA} are the constants for the formation of DP 1 from DP 4, DP 2 from DP 4, DP 3 from DP 4, DP 1 from DP 3, DP 2 from DP 3, DP 1 from DP 2, furfural from DP 1, formic acid from DP 1, and formic acid from furfural, respectively, in min^{-1}. The constants k_{FL} and k_{AL} are the constants that represent the decomposition of furfural and formic acid to loss, respectively.

during the most severe hydrolysis conditions at 200 °C 0.1 and 1 v/v% sulfuric acid, there was no DP 1 remaining after 40 min of hydrolysis. Interestingly, during hydrolysis at 200 °C 1 v/v% sulfuric acid, both furfural and formic acid were quickly degraded within 10 min of the experiment, most likely into carbon dioxide, hydrogen, carbon monoxide, water, and humins.[12−14]

The hydrolysis of furfural was conducted at the nine hydrolysis conditions used for DP 1. The survival rate of furfural after 60 min of hydrolysis ranged from 60 to 100%, with the lowest concentration of furfural remaining for the hydrolysis condition with 1 v/v% sulfuric acid at 200 °C. In most of the hydrolysis conditions, especially at 160 °C 1 v/v% sulfuric acid, a buildup of formic acid concentration was observed. In the hydrolysis condition with 1 v/v% sulfuric acid at 200 °C, 60% of the furfural remained after 60 min of hydrolysis. Furfural degradation leads to the accumulation of formic acid, which inhibits enzymatic hydrolysis, as reported by

dx.doi.org/10.1021/ie403722d | Ind. Eng. Chem. Res. XXXX, XXX, XXX−XXX

Hodge et al.[8] The hydrolysis of formic acid was similarly conducted at the nine hydrolysis conditions used for DP1. Formic acid, albeit at a slower rate, was degraded as temperature and acid concentration increased. At the most severe hydrolysis condition, 1 v/v% sulfuric acid at 200 °C, 85% of formic acid remained after 60 min of hydrolysis, as compared to the other eight hydrolysis conditions, where 93−98% of formic acid remained after 60 min of hydrolysis. Furfural formed from the autocatalytic mechanism of formic acid was not influenced by temperature or pH, as the formation rate was similar in the nine hydrolysis conditions. The detection of furfural in the hydrolyzate from the re-formation of formic acid provided the confirmation that the reaction of furfural into formic acid was indeed a reversible reaction.[14,15] However, the forward reaction of furfural to formic acid was dominant, as shown by the higher concentration of formic acid from furfural, as compared to the formation of furfural from formic acid.

Determination of Reaction Rate. All calculations were based on compound molar concentrations. The best-fit kinetic constants, k_i, are listed in Table 1; the calculated values for k_1, k_2, k_3, k_4, k_{21}, k_{31}, k_{41}, and k_{42} were 0.0054, 0.0030, 0.0103, 0.0032, 0.0030, 0.0103, 0.0001, and 0.0031 min^{-1}, respectively. Kumar and Wyman[6] reported values of 0.0059, 0.0121, 0.0240, 0.0184, 0.0059, 0.0180, 0.0148, and 0.0032 min^{-1}, respectively, for k_1, k_2, k_3, k_4, k_{21}, k_{31}, k_{41}, and k_{42}, using purified reference standards as the starting material.

Figure 6 presents the best-fit model and hydrolysis data of DP 2 as the starting material at 160 °C using 0.1 v/v% sulfuric acid. The model provided a good fit to the experimental data for the concentrations of DP 2, furfural, and formic acid concentrations but underestimated the concentration of DP 1. In order to prevent bias, the degradation rate constants were determined simultaneously for six experiments, each with different starting material, at each hydrolysis condition. Thus, the underestimation of DP 1 in one data set was offset by the overestimation of DP 1 in other data sets. This adjustment resulted in a model that best represented the experimental data. For the most part, the degradation constants calculated in this study compare favorably to the values presented by Kumar and Wyman,[6] as shown in Table 2. The discrepancy between values

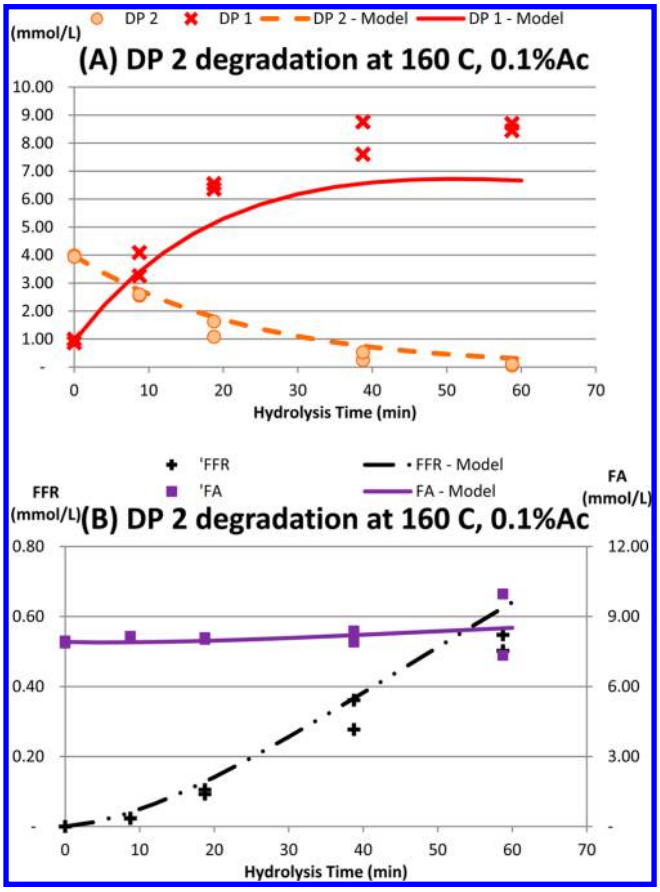

Figure 6. The best-fit model prediction and data of (A) DP 2 and DP 1 and (B) furfural (FFR) and formic acid (FA) for the hydrolysis of DP 2 at 160 °C using 0.1 v/v% sulfuric acid.

Table 2. Comparison of the Degradation Rate Constants (min^{-1}) Obtained from the Current Study and the Degradation Rate Constants Obtained from the Study by Kumar and Wyman[a]

	current study	literature
k_1	0.0054	0.0059
k_2	0.0030	0.0121
k_3	0.0103	0.0240
k_4	0.0032	0.0184
k_{21}	0.0030	0.0059
k_{31}	0.0103	0.0180
k_{41}	0.0001	0.0148
k_{42}	0.0031	0.0032

[a]Both sets of values are conducted at 160 °C using water.

was likely caused by the fact that CPC-fractionated DP 2, DP 3, and DP 4 were not of commercial grade purity and thus contained impurities, such as xylose and other oligomers, albeit at low concentrations. The calculated value of the kinetic constants k_{41} and k_{42} were used to compare the likeliness of cleaving of end bonds and middle bonds, respectively. At hydrolysis conditions of 0.1 and 1 v/v% acid at 160 °C, k_{41}/k_{42} were 2 and 384 526, respectively; these results demonstrate a strong preference for the formation of DP 1 and DP 3 from DP 4 rather than cleaving into two DP 2 units. On the other hand, cleavage of the middle bond, shown by the ratio of k_{41}/k_{42} having values of less than 1, was favored by water hydrolysis conditions; at 160 and 200 °C, ratios were calculated as 0.03 and 0.19, respectively, indicating a DP 2 formation preference from DP 4. The values obtained in this work were somewhat similar to those reported by Kumar and Wyman,[6] where the k_{41}/k_{42} ratio calculated at pH 7 was 4.63. This work, combined with that of Kumar and Wyman[6] indicated that hemicellulose-derived oligomers would not depolymerize in a homogeneous sequential fashion to DP 1 but were dependent on pH. Results in this work signify that processing parameters can affect xylose oligomer and monomer concentrations; at 160 °C acidic processing conditions will favor the production of DP 1, which will further degrade into formic acid, a potent enzymatic hydrolysis inhibitor.[8]

The assumption that the formation of formic acid from furfural was nonreversible proved valid. When furfural concentrations of 10 mmol/L were hydrolyzed in acidic conditions, formic acid concentrations of 9 mmol/L were detected after 60 min; similar reactions conducted in water yielded formic acid concentrations in the range of 1 mmol/L. On the other hand, for all hydrolysis conditions, initial formic acid concentrations of 23 mmol/L never resulted in more than 0.06 mmol/L furfural. This indicated that the reaction path of

dx.doi.org/10.1021/ie403722d | Ind. Eng. Chem. Res. XXXX, XXX, XXX−XXX

formic acid to furfural was not very favorable, greatly reducing the complexity of the model. From Table 1, the DP 1 degradation into formic acid was faster than degradation into furfural, indicating a preference in formic acid formation during DP 1 degradation. Similarly, in terms of furfural degradation, furfural rapidly degraded into formic acid, as opposed to its degradation into humin. This can be inferred by inspecting Table 1, where k_{FL}, the decomposition rate constant of furfural into humin, was smaller than k_{FA}, the decomposition rate constant for furfural into formic acid, indicating a preference of formic acid formation.

Arrhenius Parameters. The Arrhenius parameters, calculated by best-fitting the kinetic rate constants shown in Table 1, are presented in Table 3. The Arrhenius equation is shown in eq 14. The activation energies (E) of DP 1 and furfural calculated from the current study were compared to the values obtained from literature. The activation energy of DP 1 determined from the current study was comparable to the values found in the literature, while the activation energy for furfural degradation was lower than the values in the literature, but within a factor of 3,[13,19,25−28] as shown in Table 4.

Table 3. Arrhenius Parameters of the Degradation of Xylose DP 1, DP 2, DP 3, DP 4, Furfural, and Formic Acid[a]

	k_0 (min^{-1})	m (unitless)	E (kJ/mol/K)
DP 1	6.63×10^9	0.95	89.97
DP 2	8.68×10^4	1.02	37.53
DP 3	4.34×10^8	1.28	64.63
DP 4	4.43×10^7	1.57	53.01
furfural	4.26×10^3	0.09	49.55
formic acid	3.91×10^{-2}	0.01	11.82

[a] k_0, m, and E are the pre-exponential rate constant in min^{-1}, the unitless acid concentration exponent, and the activation energy in kJ/mol/K, respectively.

Table 4. Activation Energy of Xylose and Furfural in Arrhenius Equations

	feedstock	temp (°C)	xylose	furfural
Morinelly et al.[19]	switchgrass	150−175	89.0	106.0
Esteghlalian et al.[25]	switchgrass	140−180	99.5	
Jin et al.[26]	xylose	90	95.7	
Qi et al.[27]	xylose	150−200	114.4	
Weingarten et al.[13]	furfural	150−170	123.9	67.6
Rose et al.[28]	furfural	130−170		83.6
current study	birchwood xylan	120−200	90.0	49.6

Figure 7 summarizes the hydrolysis conditions for maximum xylose yield, as a function of temperature and acid concentration. Figure 7 was not presented as a function of severity index, as it was reported that this parameter was not representative with temperatures between 160 and 200 °C, as reported by Chen et al.[29] The data were determined by calculating the ratio of xylose oligomers depolymerization rate into xylose ($k_2 + k_3 + k_4$) and dividing by the degradation rate of xylose (k_1). The calculated ratios are presented as a function of temperature (x-axis) and acid concentration (y-axis). A high ratio value is desired because this indicates that the rate of xylose formation, through xylose oligomer depolymerization, is faster than the rate of xylose degradation into byproducts. Results presented in Figure 7 indicate that the optimum

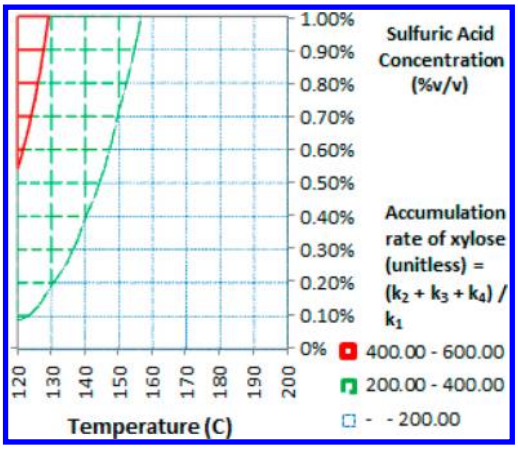

Figure 7. Kinetic model summarizing the optimum condition to maximize xylose yield. The data for the graph is calculated by determining the ratio of xylose oligomers depolymerization rate into xylose ($k_2 + k_3 + k_4$) and dividing by the degradation rate of xylose (k_1). A high value (as represented by the solid line region) is desired.

hydrolysis temperatures of in-house-produced oligomers were between 120 and 130 °C and acid concentrations greater than 1 v/v%. Similarly, on the basis of the model developed in this study, high temperature and low acid conditions, such as using a water-only hydrolysis condition, were not desirable because they did not favor oligomer depolymerization into xylose as compared to the rate of xylose degradation, resulting overall in low xylose accumulation.

Figure 8 presents the degradation rate of xylose, k_1, as a function of temperature (x-axis) and acid concentration (y-axis). Mild hydrolysis conditions are preferred to minimize the accumulation of byproducts, such as furfural and formic acid. Byproducts formed from degraded xylose cannot be easily removed and negatively affect subsequent enzymatic hydrolysis and fermentation processes. Therefore, the optimum hydrolysis condition should minimize the degradation rate of xylose, k_1. On the basis of the model developed in the current study, temperatures below 170 °C minimized xylose degradation. Thus, based on the analysis of Figures 7 and 8, the optimum hydrolysis conditions consisted of low temperatures (120−130

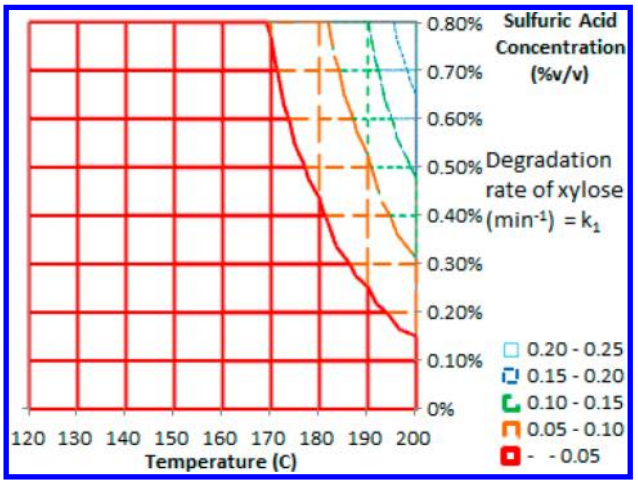

Figure 8. Kinetic model summarizing the optimum condition to minimize xylose degradation. The data for the graph is based on the degradation rate of xylose (k_1). A low value (as represented by the solid line region) is desired.

dx.doi.org/10.1021/ie403722d | Ind. Eng. Chem. Res. XXXX, XXX, XXX−XXX

°C) and high acid concentrations (0.6−1.0 v/v%), which favored xylose accumulation but minimized its degradation into byproducts.

However, at low temperature, the depolymerization rate of xylose oligomers into xylose will be slower and, thus, result in longer hydrolysis time and higher production cost through the use of larger volume reactors. Figure 9 presents the depolymerization rate of xylose oligomers. As predicted, xylose oligomers degraded faster at higher temperatures. For example, the degradation rate of xylose oligomers increased by more than 4 times when the hydrolysis temperature was raised from 120 to 160 °C and by more than 6 times when the temperature was raised to 170 from 120 °C. In comparison, xylose accumulation rates were reduced by 3-fold when the temperature was increased from 120 to 160 °C and by close to 4-fold when the temperature was raised to 170 from 120 °C. Figures 7−9 were prepared on the basis of the Arrhenius parameters and could provide valuable information for setting up two-stage hydrolysis processes, as reported by Grohman and Torget.[30] Careful trade-offs must be made between reaction rate, xylose accumulation rate, and xylose degradation rate, as well as innate biomass buffering capacity, in order to maximize xylose yields, at a reasonable cost.

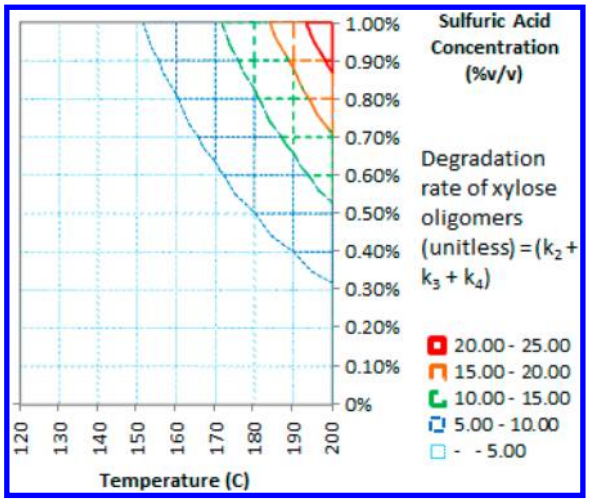

Figure 9. Kinetic model summarizing the reaction rate. The data for the graph is calculated by determining the xylose oligomers depolymerization rate into xylose ($k_2 + k_3 + k_4$). A high value (as represented by the solid line region) is desired.

CONCLUSION

Current work determined the kinetic rate of individual oligomers and degradation compounds, which is an approach that has not been conducted in previous studies. Moreover, current study utilized birchwood-xylan purified xylose oligomers, which is a step bearing more resemblance to biomass hydrolysis systems. On the basis of the tested oligomer system, the highest xylose concentrations were obtained at low temperature and high acid concentration. Byproduct formation was minimized at low temperature and acid concentration. Since, once formed, byproducts do not degrade as easily as compared to oligomers and impede enzymatic hydrolysis, their generation should be minimized. Unfortunately the pretreatment step cannot be omitted; therefore, processing trade-offs must be implemented, such that xylose is released with minimal byproduct generation.

AUTHOR INFORMATION

Corresponding Author

*Telephone: ++1 479 575 2351. Fax: ++1 479 575 2846. E-mail: carrier@uark.edu.

Notes

The authors declare no competing financial interest.

ACKNOWLEDGMENTS

The authors gratefully acknowledge financial support from the University of Arkansas, the National Science Foundation (award #0828875), the U.S. Department of Energy (award #08GO88036), the CSREES National Research Initiative (award #2008-01499), and The Plant Powered Production (P3) Center, which is funded wholly or in part by the National Science Foundation (NSF) EPSCoR Program and the Arkansas Science & Technology Authority (award # EPS-1003970). The authors would also like to thank Dr. Kris Bunnell, Mr. Chris McDaniel, Dr. Betty Martin, Dr. Jin-Woo Kim, and Dr. Tom Costello for their assistance in various stages of the project.

REFERENCES

(1) Brodeur, G.; Yau, E.; Badal, K.; Collier, J.; Ramachandran, K.; Ramakrishnan, S. Chemical and Physicochemical Pretreatment of Lignocellulosic Biomass: A Review. *Enzyme Res.* **2011**, DOI: 10.4061/2011/787532.

(2) Mosier, N.; Wyman, C.; Dale, B.; Elander, R.; Lee, Y.; Holtzapple, M.; Ladisch, M. Features of Promising Technologies for Pretreatment of Lignocellulosic Biomass. *Bioresour. Technol.* **2005**, *96*, 673−686.

(3) Yang, B.; Wyman, C. E. Pretreatment: The Key to Unlocking Low-Cost Cellulosic Ethanol. *Biofuels Bioprod. Biorefin.* **2008**, *2*, 26−40.

(4) Kumar, R.; Wyman, C. Effect of Enzyme Supplementation at Moderate Cellulase Loadings on Initial Glucose and Xylose Release from Corn Stover Solids Pretreated by Leading Technologies. *Biotechnol. Bioeng.* **2009**, *102*, 457−467.

(5) Samala, A.; Srinivasan, R.; Yadav, M. P.; Kim, T.; Prewitt, L. Xylo-Oligosaccharides Production by Autohydrolysis of Corn Fiber Separated from DDGS. *BioResources* **2012**, *7*, 3038−3050.

(6) Kumar, R.; Wyman, C. E. The Impact of Dilute Sulfuric Acid on the Selectivity of Xylooligomer Depolymerization to Monomers. *Carbohydr. Res.* **2008**, *343*, 290−300.

(7) Nimlos, M. R.; Qian, X.; Davis, M.; Himmel, M. E.; Johnson, D. K. Energetics of Xylose Decomposition as Determined Using Quantum Mechanics Modeling. *J. Phys. Chem. A* **2006**, *110*, 11824−11838.

(8) Hodge, D. B.; Karim, M. N.; Schell, D. J.; McMillan, J. D. Soluble and Insoluble Solids Contributions to High-Solids Enzymatic Hydrolysis of Lignocellulose. *Bioresour. Technol.* **2008**, *99*, 8940−8948.

(9) Ximenes, E.; Kim, Y.; Mosier, N.; Dien, B.; Ladisch, M. Inhibition of Cellulases by Phenols. *Enzyme Microb. Technol.* **2010**, *46*, 170−176.

(10) Palmqvist, E.; Hahn-Hägerdal, B. Fermentation of Lignocellulosic Hydrolysates. II, Inhibitors and Mechanisms of Inhibition. *Bioresour. Technol.* **2000**, *74*, 25−33.

(11) Qing, Q.; Wyman, C. E. Hydrolysis of Different Chain Length Xylooliogmers by Cellulase and Hemicellulase. *Bioresour. Technol.* **2011**, *102*, 1359−1366.

(12) O'Neill, R.; Ahmad, M. N.; Vanoye, L.; Aiouache, F. Kinetics of Aqueous Phase Dehydration of Xylose into Furfural Catalyzed by ZSM-5 Zeolite. *Ind. Eng. Chem. Res.* **2009**, *48*, 4300−4306.

(13) Weingarten, R.; Cho, J.; Conner, W. C.; Huber, G. W. Kinetics of Furfural Production by Dehydration of Xylose in a Biphasic Reactor with Microwave Heating. *Green Chem.* **2010**, *12*, 1423−1429.

(14) Dias, A. S.; Pillinger, M.; Valente, A. A. Dehydration of Xylose into Furfural over Micro−Mesoporous Sulfonic Acid Catalysts. *J. Catal.* **2005**, *229*, 414−423.

(15) Antal, M.; Leesomboon, T.; Mok, W.; Richards, G. Mechanism of Formation of 2-Furaldehyde from D-Xylose. *Carbohydr. Res.* **1991**, *217*, 71−85.
(16) Yu, J.; Savage, P. E. Decomposition of Formic Acid under Hydrothermal Conditions. *Ind. Eng. Chem. Res.* **1998**, *37*, 2−10.
(17) Akiya, N.; Savage, P. E. Role of Water in Formic Acid Decomposition. *AIChE J.* **1998**, *44*, 405−415.
(18) Kamiyama, Y.; Sakai, Y. Kinetics of Diluted Acid Hydrolysis of Hardwood Xylan. *J. Agric. Chem. Soc. Jpn.* **1984**, *12*, 1211−1216.
(19) Morinelly, J. E.; Jensen, J. R.; Browne, M.; Co, T. B.; Shonnard, D. R. Kinetic Characterization of Xylose Monomer and Oligomer Concentrations during Dilute Acid Pretreatment of Lignocellulosic Biomass from Forests and Switchgrass. *Ind. Eng. Chem. Res.* **2009**, *48*, 9877−9884.
(20) Kim, Y.; Kreke, T.; Ladisch, M. R. Reaction Mechanisms and Kinetics of Xylo-Oligosaccharide Hydrolysis by Dicarboxylic Acids. *AIChE J.* **2013**, *59*, 188−199.
(21) Lau, C. S.; Clausen, E. C.; Lay, J. O.; Gidden, J.; Carrier, D. J. Separation of Xylose Oligomers Using Centrifugal Partition Chromatography with a Butanol−Methanol−Water System. *J. Ind. Microbiol. Biotechnol.* **2013**, *40*, 51−62.
(22) Djioleu, A.; Arora, A.; Martin, E.; Smith, J.; Pelkki, M.; Carrier, D. Sugar Recovery from the Pretreatment/Enzymatic Hydrolysis of High and Low Specific Gravity Poplar Clones. *Agric. Food Anal. Bacteriol.* **2012**, *2*, 121−131.
(23) Martin, E.; Duke, J.; Pelkki, M.; Clausen, E. C.; Carrier, D. J. Sweetgum (*Liquidambar styraciflua L.*): Extraction of Shikimic Acid Coupled to Dilute Acid Pretreatment. *Appl. Biochem. Biotechnol.* **2010**, *162*, 1660−1668.
(24) Saeman, J. F. Kinetics of Wood Saccharification−Hydrolysis of Cellulose and Decomposition of Sugars in Dilute Acid at High Temperature. *Ind. Eng. Chem.* **1945**, *37*, 43−52.
(25) Esteghlalian, A.; Hashimoto, A. G.; Fenske, J. J.; Penner, M. H. Modeling and Optimization of the Dilute-Sulfuric-Acid Pretreatment of Corn Stover, Poplar and Switchgrass. *Bioresour. Technol.* **1997**, *59*, 129−136.
(26) Jin, Q.; Zhang, H.; Yan, L.; Qu, L.; Huang, H. Kinetic Characterization for Hemicellulose Hydrolysis of Corn Stover in a Dilute Acid Cycle Spray Flow-through Reactor at Moderate Conditions. *Biomass Bioenergy* **2011**, *35*, 4158−4164.
(27) Qi, W.; Zhang, S. P.; Xu, Q. L.; Ren, Z. W.; Yan, Y. J. Degradation Kinetics of Xylose and Glucose in Hydrolysate Containing Dilute Sulfuric Acid. *Chin. J. Process Eng.* **2008**, *8*, 1132−1137.
(28) Rose, I. C.; Epstein, N.; Watkinson, A. P. Acid-Catalyzed 2-Furaldehyde (Furfural) Decomposition Kinetics. *Ind. Eng. Chem. Res.* **2000**, *39*, 843−845.
(29) Chen, S. F.; Mowery, R. A.; Chambliss, C. K.; van Walsum, G. P. Pseudo Reaction Kinetics of Organic Degradation Products in Dilute-Acid-Catalyzed Corn Stover Pretreatment Hydrolysates. *Biotechnol. Bioeng.* **2007**, *6*, 1135−1145.
(30) Grohmann, K.; Torget, R. W. Two-Stage Dilute Acid Prehydrolysis of Biomass. US Patent 5125977, 1992.